Msl1-Mediated Dimerization of the Dosage Compensation Complex Is Essential for Male X-Chromosome Regulation in *Drosophila*

Erinc Hallacli,[1,4] Michael Lipp,[2,3,4] Plamen Georgiev,[1] Clare Spielman,[1] Stephen Cusack,[2,3] Asifa Akhtar,[1,*] and Jan Kadlec[2,3,*]
[1]Max-Planck-Institut für Immunbiologie und Epigenetik, Stübeweg 51, 79108 Freiburg im Breisgau, Germany
[2]European Molecular Biology Laboratory, Grenoble Outstation
[3]Unit of Virus Host-Cell Interactions, UJF-EMBL-CNRS, UMI 3265
6 rue Jules Horowitz, BP181, 38042 Grenoble Cedex 9, France
[4]These authors contributed equally to this work
*Correspondence: akhtar@ie-freiburg.mpg.de (A.A.), kadlec@embl.fr (J.K.)
http://dx.doi.org/10.1016/j.molcel.2012.09.014

SUMMARY

The Male-Specific Lethal (MSL) complex regulates dosage compensation of the male X chromosome in *Drosophila*. Here, we report the crystal structure of its MSL1/MSL2 core, where two MSL2 subunits bind to a dimer formed by two molecules of MSL1. Analysis of structure-based mutants revealed that MSL2 can only interact with the MSL1 dimer, but MSL1 dimerization is MSL2 independent. We show that Msl1 is a substrate for Msl2 E3 ubiquitin ligase activity. ChIP experiments revealed that Msl1 dimerization is essential for targeting and spreading of the MSL complex on X-linked genes; however, Msl1 binding to promoters of male and female cells is independent of the dimer status and other MSL proteins. Finally, we show that loss of Msl1 dimerization leads to male-specific lethality. We propose that Msl1-mediated dimerization of the entire MSL complex is required for Msl2 binding, X chromosome recognition, and spreading along the X chromosome.

INTRODUCTION

Heterogametic organisms with unequal numbers of sex chromosomes have to go through a process called dosage compensation to equilibrate their transcriptional output. Diverse solutions to the dosage problem evolved in different organisms. *Drosophila melanogaster* males transcriptionally upregulate their single X chromosome roughly two times to compensate for the absence of an active homolog (Conrad and Akhtar, 2011), whereas in mammals, females inactivate one of the two X chromosomes (Augui et al., 2011). Dosage compensation not only balances sex differences, but has also been shown to equalize X to autosome ratios in mammals, *C. elegans*, and *Drosophila* (Deng et al., 2011; Kharchenko et al., 2011). Dosage compensation mechanisms provide an excellent model for studying chromosome-wide transcription regulation through epigenetic mechanisms (Gelbart and Kuroda, 2009).

In *Drosophila*, the Male-Specific Lethal (MSL) complex, also known as the dosage-compensation complex (DCC), mediates dosage compensation (Hallacli and Akhtar, 2009). The complex consists of at least five MSL proteins (Msl1, Msl2, Msl3, Maleless [Mle], and Males-absent-on-the-first [Mof]) and two redundant long noncoding RNAs (roX1 and roX2) (Ilik and Akhtar, 2009). An equivalent, highly conserved complex also exists in human, composed of at least MSL1, MSL2, MSL3, and MOF. Whether any noncoding RNAs reside in the mammalian MSL complex remains unknown (Marín, 2003; Smith et al., 2005; Kadlec et al., 2011; Wu et al., 2011). MSL1, predicted to contain no globular domains, serves as a scaffold of the MSL complex (Kadlec et al., 2011). It interacts with its conserved C-terminal region, called the PEHE domain, with the histone acetyltransferases (HAT) domain of MOF and the MRG domain of MSL3 (Kadlec et al., 2011). Both *Drosophila* and human MSL1 were proposed to interact with MSL2 via an N-terminal predicted coiled-coil region (Li et al., 2005; Wu et al., 2011). MSL2 consists of an N-terminal RING finger and a C-terminal cysteine-rich domain involved in DNA binding (Fauth et al., 2010). The best-studied catalytic activity of the complex is the MOF-mediated acetylation of histone H4 at lysine 16 (H4K16ac) on the X chromosome (Hilfiker et al., 1997; Akhtar and Becker, 2000; Smith et al., 2000). We have recently shown that Mof's enzymatic activity is tightly regulated for H4K16 acetylation, promoting enhanced loading of RNAPII at the promoters of X-linked genes (Conrad et al., 2012a, 2012b). Human MSL2 has also been shown to be an E3 ubiquitin ligase for lysine 34 of histone H2B (Wu et al., 2011), suggesting that other histone marks may crosstalk on the male X chromosome.

According to the current model, the MSL complex is first enriched on numerous GA repeat-rich sequences called high-affinity sites (HAS), such as roX genes, followed by spreading to the rest of the X chromosome in a sequence-independent manner (Alekseyenko et al., 2008). Interestingly, HAS can be qualitatively differentiated with respect to their requirement of either Msl3 or Mof and their genomic location (Kadlec et al., 2011).

To gain mechanistic insights into how Msl1 and Msl2 influence dosage compensation, we determined the crystal structure of
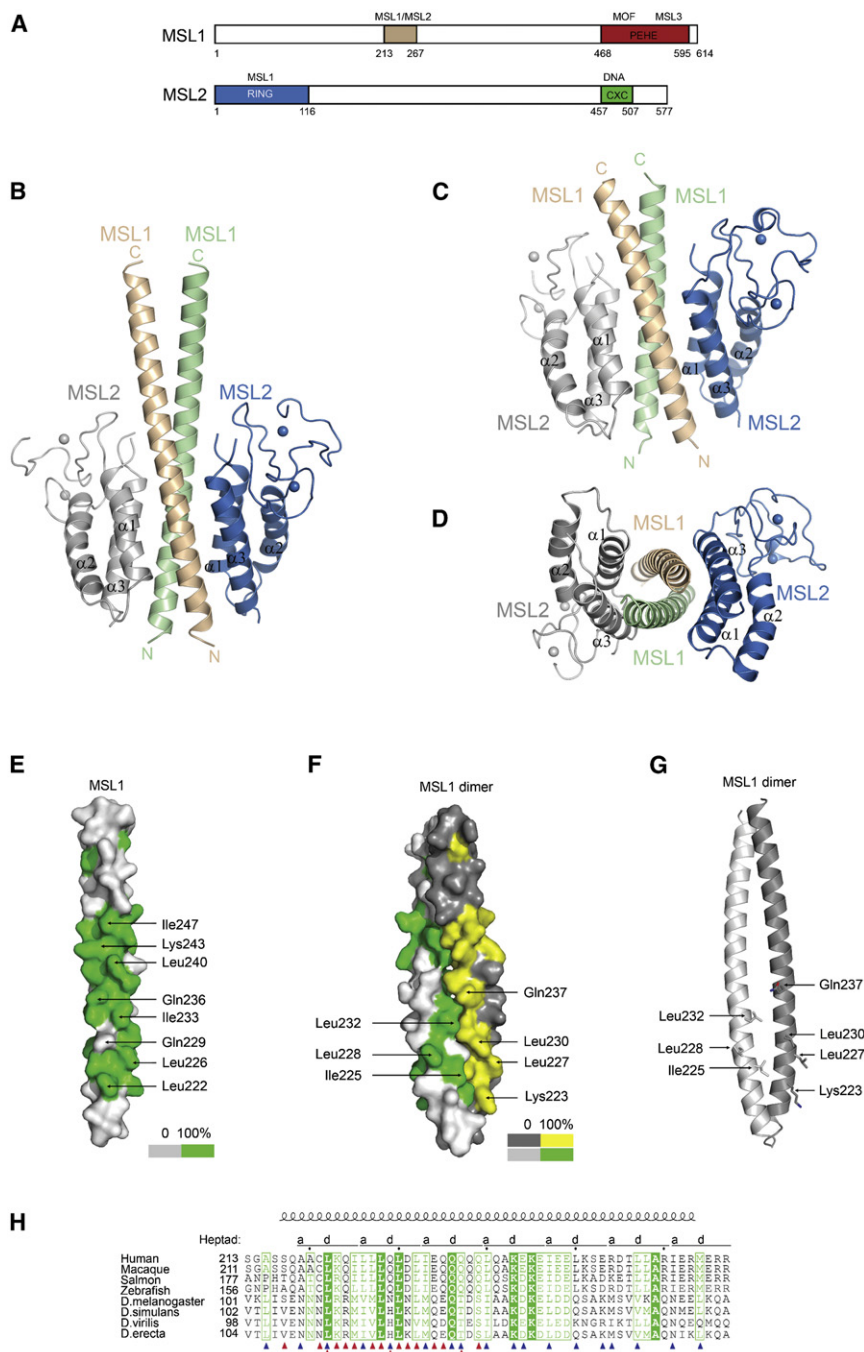
Figure 1. Crystal Structures of the MSL1/MSL2 Complex

(A) Schematic representation of the domain structures of human MSL1 and MSL2. The binding partners are indicated above individual domains.

(B) Ribbon diagram of the human MSL1$_{213-267}$/MSL2$_{1-116}$ complex. Two molecules of MSL1 form the central dimeric coiled coil (shown in brown and green). The N-terminal RING finger-containing domains of MSL2 are shown in blue and gray.

(C) Ribbon representation of the complex between shorter MSL1$_{213-252}$ and MSL2$_{1-116}$ in the same orientation as in (A).

(D) The MSL1$_{213-252}$/MSL2$_{1-116}$ structure rotated by 90° along the horizontal axis relative to (C).

(E) Surface representation of the MSL1 helix. Conserved surface residues, based on the sequence alignment in (H), are shown in green, indicating 100% conservation. Only conserved residues involving MSL1 dimerization are labeled.

(F) Surface representation of the MSL1 dimer forming composite binding sites for MSL2. Highly conserved residues are shown in green and yellow and residues binding MSL2 are labeled. Gln237 is also highlighted; as in *Drosophila*, its substitution with threonine is compensated by T7Q mutation in Msl2.

(G) Ribbon representation of the MSL1 dimer in the same orientation as in (F), showing the conserved MSL2 binding residues.

(H) Sequence alignment of MSL1 proteins comparing vertebrates and *Drosophila* species. Only the sequence of the coiled-coil region is shown. Identical residues are in green boxes, and conserved residues are shown in green. Blue triangles indicate residues involved in the MSL1 dimerization while red triangles show residues interacting with MSL2.

Msl1 dimerization plays a vital role in vivo, as specific point mutations lead to male-specific lethality in flies.

RESULTS

MSL1 and MSL2 Form a Heterotetrameric Core of the MSL Complex

The complex between the predicted coiled-coil region of human MSL1 (residues 213–326) and the N-terminal portion of MSL2 (residues 1–116) was formed by

the complex between their highly conserved human orthologs, which unexpectedly show that MSL1 and MSL2 form a heterotetrameric core of the MSL complex. Functional experiments with structure-based *Drosophila* Msl1 mutants revealed that Msl1 dimerization is required for Msl2 and roX2 RNA binding, X chromosome recognition, and spreading along the X chromosome. Furthermore, we established a dimerization-, Msl2-, Msl3-, and Mof-independent binding of Msl1 at autosomal and X-linked promoters of male and female cells. Finally, we show that the

coexpression in bacteria. Using trypsin-limited proteolysis, we identified a shorter MSL1 fragment spanning residues 213–267 that was sufficient for the MSL2 binding. The structure of this complex was determined by X-ray crystallography at a resolution of 3.5 Å (Figure 1). In order to improve the crystal quality, the MSL1 fragment was further shortened to residues 213–252, and a structure of its complex with MSL2$_{1-116}$ was solved at 3.25 Å resolution and refined to an R factor of 24.4% and R$_{free}$ of 26% (Figures 1C and 1D). Msl1 and Msl2 proteins were

originally suggested to dimerize via their putative coiled-coil regions (Scott et al., 2000; Li et al., 2005). However, unexpectedly, both of our structures show that instead these two proteins form a heterotetrameric core of the MSL complex, where two MSL1 subunits form a dimeric coiled coil that serves as a binding platform for two molecules of MSL2 (Figure 1). Additionally, we confirmed by multiangle laser light scattering (MALLS) that the MSL1/MSL2 subcomplex has an apparent 2:2 stoichiometry also in solution (Figures S1A and S1B).

The MSL1-MSL1 Interface

The crystallized fragment of MSL1 (residues 213–267) forms a 75 Å long parallel dimeric coiled coil, where ten hydrophobic and four polar residues (Gln229, Gln236, Lys243, and Arg254), originally thought to be involved in the interaction with MSL2 (Li et al., 2005), pack in layers with a regular heptad (3–4) periodicity (Figures 1E–1H, S1C, and S1D). Additional stabilizing interactions between the helices are shown in Figure S1D. The dimer's two Glu229 and Glu236 residues form interhelical hydrogen bonds at its core (Figure S1D). The predicted heptad repeats in human MSL1 extend until residue 285, suggesting the MSL1-MSL1 coiled coil might be even longer. However, mass spectrometry analysis of a tryptic digest of the MSL1$_{213-310}$-containing complex revealed four sites accessible to trypsin at positions 266, 267, 272, and 273, indicating that this possible extension is less stable than the crystallized segment (Figures S1E and S1F). The heptad pattern between residues 215 and 233 was difficult to predict, as this region also contains a cluster of hydrophobic residues involved in the interaction with the helices of MSL2 (Figure 1H). A corresponding coiled coil in *Drosophila* Msl1 is located closer to the N terminus than in the human protein and is predicted to be longer (residues 100–176). We showed that Msl1$_{85-186}$ forms a stable complex with Msl2$_{1-192}$ in vitro (Figure S2A). Most of the residues involved in the MSL1 dimerization are highly conserved across species, reflecting the importance of this interaction for the functional integrity of the MSL complex (Figures 1E and 1H). Upon dimerization, the MSL1 coiled coil forms two composite, mostly hydrophobic binding sites for two molecules of MSL2, which are clearly identifiable by mapping of conserved residues onto the surface of the dimer (Figures 1F and 1G).

The Structure of MSL2

The structure of the N-terminal region of MSL2 consists of three long helices (α1, α2, and α3) forming a triple-stranded antiparallel coiled coil and a RING finger that is inserted between helix α2 and α3 (Figure 2A). MSL2$_{1-116}$ exhibits a sequence similarity to the N-terminal domain of BRCA1 ubiquitin ligase, mostly within the helix α2 and the RING finger. Superposition of the BRCA1 structure (PDB code 1JM7) onto MSL2 revealed that these two domains are indeed similar (Figures 2A and 2B; RMS deviation 2.1 Å for 77 Cα atoms). In the BRCA1 structure, the central RING finger is flanked only by two helices, corresponding to α2 and α3 of MSL2, which form a four-helix bundle with corresponding helices of BARD1 (Brzovic et al., 2001). Interestingly, in MSL2, the packing of helix α1 against helices α2 and α3 resembles the C-terminal helix of BARD1 binding to BRCA1 (Figures 2C and 2D). The MSL1 binding surface is then formed by helices α1 and α3.

The RING finger of MSL2 includes residues 42–93 and adopts a fold observed in other RING domain structures. The two Zn atoms are coordinated by absolutely conserved Cys44, Cys47, Cys67, and Cys70 and Cys62, His64, Cys81, and Cys84, respectively (Figure S2B). The N-terminal portion of the RING finger, which is in proximity of the helices of MSL2, is stabilized by interactions between conserved Leu50, which points toward a hydrophobic cavity between helices α2 and α3, and Gln63, which forms several hydrogen bonds with Val4 and Asn5 of α1. A solvent-exposed loop binding the second Zn atom (71–90) is the most flexible and poorly defined in both structures.

Human MSL2 was reported to be an E3 ligase for p53 and its RING finger to be indispensable for this activity (Kruse and Gu, 2009). Recently, MSL2 has been shown to ubiquitinate histone H2B, and its activity was greatly reduced by H64Y mutation within the RING finger (Wu et al., 2011). We thus analyzed the MSL2 RING finger structure with respect to its role in ubiquitination. The structure of c-Cbl in a complex with UbcH7 serves as a model for interactions between RING domains with E2 enzymes (Zheng et al., 2000). Ile383, Trp408, Pro417, and Phe418 of c-Cbl and equivalent residues in other RING proteins make a largely hydrophobic interacting surface contacting two loops of E2 (Figure 2E). Surprisingly, a corresponding interaction surface is not formed in the MSL2 structure. MSL2 lacks the central helix (downstream of Cys70) that is characteristic for most RING finger domains and that normally forms the E2 binding groove (Figures 2E–2G). Instead, a loop (residues 71–77) binds across the putative E2 binding surface, with Val46, Met75, and Met77 being buried in the interface (Figure 2F). This unusual conformation might be a result of the crystallization process, which would be in agreement with the high flexibility of this region seen in this and other RING structures. However, a similar positioning of this loop occurs also in the structure of promyelocytic leukemia proto-oncoprotein PML that equally lacks the central helix (buried Met38; Figure 2G) (Borden et al., 1995). Alternatively, this structure might represent an autoinhibited state of the RING finger, as recently characterized for TRAF2. This protein has an insertion in the loop that would apparently inhibit E2 binding; however, upon binding of a cofactor, TRAF2 is nevertheless active (Alvarez et al., 2010). It seems unlikely that the MSL2 RING finger could interact with an E2 in a way similar to other E3 enzymes without a local conformational change of the 71–77 loop that would make accessible the putative E2 binding surface (Figure S2C).

We tested the ubiquitination activity of *Drosophila* Msl2 using purified full-length protein expressed in insect cells in an in vitro ubiquitination assay (Figure 2H). In agreement with the literature, we could show that Msl2 can autoubiquitinate itself, which is a hallmark of E3 ligase proteins (Figure 2I). Msl1 did not exhibit any ubiquitination activity (data not shown). Interestingly, in the presence of the Msl2/Msl1 complex, both Msl1 and Msl2 were ubiquitinated, as the amount of unmodified proteins was rapidly decreasing in time (Figure 2J). This experiment indicates that Msl1 is a substrate of Msl2 in vitro and that the Msl1/Msl2 tetramer has significantly higher activity compared to Msl2 alone (Figures 2I and 2J). The increased activity of Msl1/Msl2 tetramer was also observed on Rpn10, a universal substrate for E3 ligases (Uchiki et al., 2009) (Figure S2F). Similarly, human MSL1/MSL2
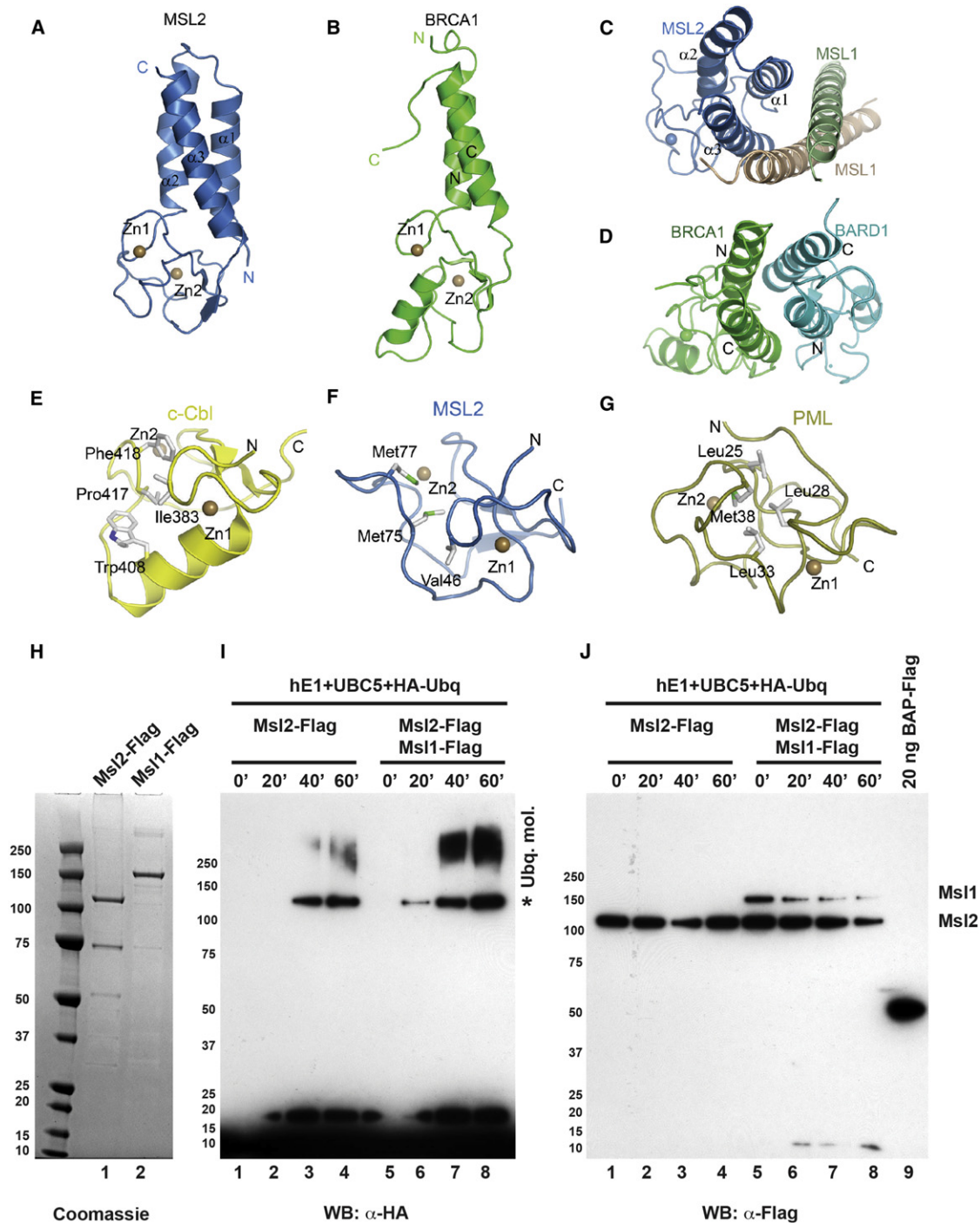
Figure 2. Structure of the N-Terminal Domain of MSL2 and Its Ubiquitination Activity

(A) Ribbon representation of the MSL2$_{1-116}$ structure. A RING finger coordinating two zinc atoms is inserted between helices α2 and α3.

(B) The MSL2 RING finger-containing domain is similar to the N terminus of BRCA1 (PDB code 1JM7).

(C and D) Comparison of the MSL1/MSL2 and BRCA1/BARD1 complexes. MSL2 interacts with MSL1 with α1 and α3 (C). Helix α1 of MSL2 packs against helices α2 and α3 in position equivalent to the one of the C-terminal helix of BARD1 interacting with BRCA1 (D).

(E) RING finger of c-Cbl (PDB code 1FBV). Ile383, Trp408, Pro417, and Phe418 form a hydrophobic groove involved in the interaction with UbcH7 E2 enzyme.

(F) RING finger of MSL2 (residues 42–93). Loop 71–77 binds across the putative E2 binding site.

(G) RING finger of promyelocytic leukemia proto-oncoprotein PML (PDB code 1BOR). The E2 binding site is obstructed in a way similar to MSL2.

(H) SDS-PAGE gel showing the purified *Drosophila* Msl1-Flag and Msl2-Flag expressed in insect cells. In lane 1, the 75 kDa band is a common contaminant of Msl2 purifications and 50 kDa band is a degradation product of Msl2.

has higher ubiquitination activity than MSL2 alone (Wu et al., 2011). We propose that this increased activity is achieved via Msl1-mediated dimerization of Msl2, which is in line with often-observed activity boost of E3 ubiquitin ligase dimers compared to monomers (Budhidarmo et al., 2012).

To understand the importance of the E3 ligase activity of Msl2, we prepared several mutations aimed to disrupt its interaction with E2 enzymes. We observed that triple mutation of the *Drosophila* counterparts of Val46, Met75, and Met77 of the loop occluding the putative E2 binding surface (Val43, Lys72, and Met74), but not single mutants, significantly reduced Msl2 E3 activity (Figures S2G and S2H). These mutations, however, also affected the overall Msl2 structure, as this mutant no longer interacted with Msl1 (Figure S2I).

The MSL1/MSL2 Interface

Msl2 was suggested to interact with Msl1 via its RING finger (Copps et al., 1998). In contrast, our structure shows that its interaction with the MSL1 dimer is exclusively mediated by helices α1 and α3, while the RING finger has no contact with MSL1. Interestingly, the putative role of the *Drosophila* Msl2 RING finger in the interaction with Msl1 was established by identification of 13 mutations, which in light of the present structure would nearly all destabilize the RING finger and thus probably also the entire Msl2 (Copps et al., 1998). Only two of these mutations (M14K and C107R) would probably directly affect the binding of helix α1 and α3 to Msl1. The helices of the two MSL2 molecules bind to MSL1 in an antiparallel fashion, forming an eight-helical bundle (Figure 3A) with multiple contacts within several hydrophobic and polar layers along the first three heptad repeats of MSL1. The complex interface buries 1180 $Å^2$ of the MSL1 dimer. The key interacting residues of MSL1 form a short, highly conserved cluster between Ser117 and Gln239 (Figures 1F–1H). The interacting residues of MSL2 are highlighted in Figure S2B and include conserved Tyr10, Arg15, Gln95, Cys102, and Tyr109. At the N-terminal end of MSL1, Ser117 forms a hydrogen bond with Gln112 of MSL2. Above, a mixed hydrophobic-polar layer is formed around MSL1 Leu222, where Cys221, Lys223, and Gln224 make several hydrogen bonds with Lys105, Glu108, and Tyr109 of α3 of MSL2 (Figure 3C). The central polar layer formed around MSL1 Gln229 and MSL2 Tyr10 (Figure 3D) is isolated on both sides from solvent by numerous hydrophobic residues of MSL1 and MSL2. Finally, the glutamine cluster at heptad 3, including Gln236 and Gln237, forms a network of hydrogen bonds with MSL2 (Figure 3B). The helical bundle is stabilized also on the exterior by salt bridges between Arg15 of MSL2 and Asp231 and Glu234 of MSL1.

In *Drosophila* Msl1 the important Gln237 is replaced by a threonine. Interestingly, Msl2 contains a compensatory threonine to glutamine mutation that might preserve the hydrogen bonding. The interaction network in the *Drosophila* complex is also likely to be maintained by L99Q mutation that compensates

for Gln95 substitution for a methionine (Figures S2D and S2E). Thus, even though the level of conservation of the MSL1 coiled-coil region between human and *Drosophila* appears to be lower than in the case of the MSL3 and MOF binding regions (Kadlec et al., 2011), we believe the structure of the MSL1/MSL2 heterotetramer is very similar between these two species.

MSL1 Dimerization and MSL2 Binding Can Be Separated

Since the role of the MSL complex is better understood in *Drosophila*, and the key residues in all interaction interfaces MSL1 makes with MSL1, MSL2, MSL3, and MOF are evolutionarily conserved, we performed all our functional studies with *Drosophila* proteins in cell lines as well as transgenic flies. All the *Drosophila* Msl1 mutants used in this study and the corresponding mutations to mammalian counterparts are summarized in Figure 3E, and they all have a C-terminal 3xFlag epitope unless indicated otherwise.

In our previous study, we showed that the Msl3 and Mof interactions with Msl1 can be disrupted without any apparent influence on the other protein-protein interactions within the complex (Kadlec et al., 2011). To further support this finding and functionally separate the N-terminal interactions of Msl1 with Msl2 and the C-terminal interactions with Mof and Msl3 (through the PEHE region), we generated an Msl1 mutant (Msl1 mut.1) that binds neither Msl3 nor Mof (Figure 3F, lane 2, see also Figure S3A). Using coimmunoprecipitation with transiently expressed Msl1, we could show that the Msl1 interaction with Msl2 remains unaffected even when both Msl3 and Mof are eliminated from the complex (Figure 3F).

To test the dimerization of the full-length Msl1 in vivo, we transiently coexpressed the wild-type (WT) Msl1-Flag and Msl1-myc proteins and immunoprecipitated Msl1-Flag proteins using a Flag antibody-coupled resin. Indeed, the Flag-tagged Msl1 coimmunoprecipitated with Msl1-myc as well as Msl2, Msl3, and Mof (Figure 3F lane 1). Furthermore, we observed that Msl1 can dimerize even in the absence of Msl3 and Mof (Figure 3F lane 2). Next, we were interested in identifying Msl1 mutations that would disrupt its dimerization, without directly affecting the residues interacting with Msl2. Thus, we mutated either four or five residues at *a* or *d* heptad positions along the coiled coil to aspartates (Msl1 mut.2 and mut.3; Figures 1E, 1H, and 3E). Both mutants, although they were highly expressed, failed to copurify Msl1-myc and Msl2, while the interaction with Msl3 and Mof was unaffected (Figure 3F, lane 3 and 4). This experiment confirms that the interaction with Msl2 requires the entire composite Msl2 binding site formed by the Msl1 dimer (Figure 3A). We cannot exclude that the presence of two aspartate side chains (V114D, M121D) might affect the Msl1/Msl2 interface directly. It is important to note that neither the Msl1 dimerization nor Msl2 binding is required for the interaction with Msl3 and Mof. These results emphasize the modular nature of Msl1 interactions with different members of the MSL complex.

(I) In vitro ubiquitination assay with recombinant Flag-tagged Msl1 and Msl2. Equal amounts of proteins were assayed in 20 min time interval. HA antibody was used to determine the autoubiquitination of Msl2 (lanes 1–4) and ubiquitinated species of Msl1 and Msl2 (lanes 5–8). 0 time point indicates no ATP control. Asterisk indicates E1 enzyme ubiquitination.

(J) The same experiment as in (I) blotted for Flag antibody to monitor Msl1 and Msl2 species. Twenty nanograms BAP-Flag protein is used as an indicator of the amounts of Msl1 and Msl2 in this assay.
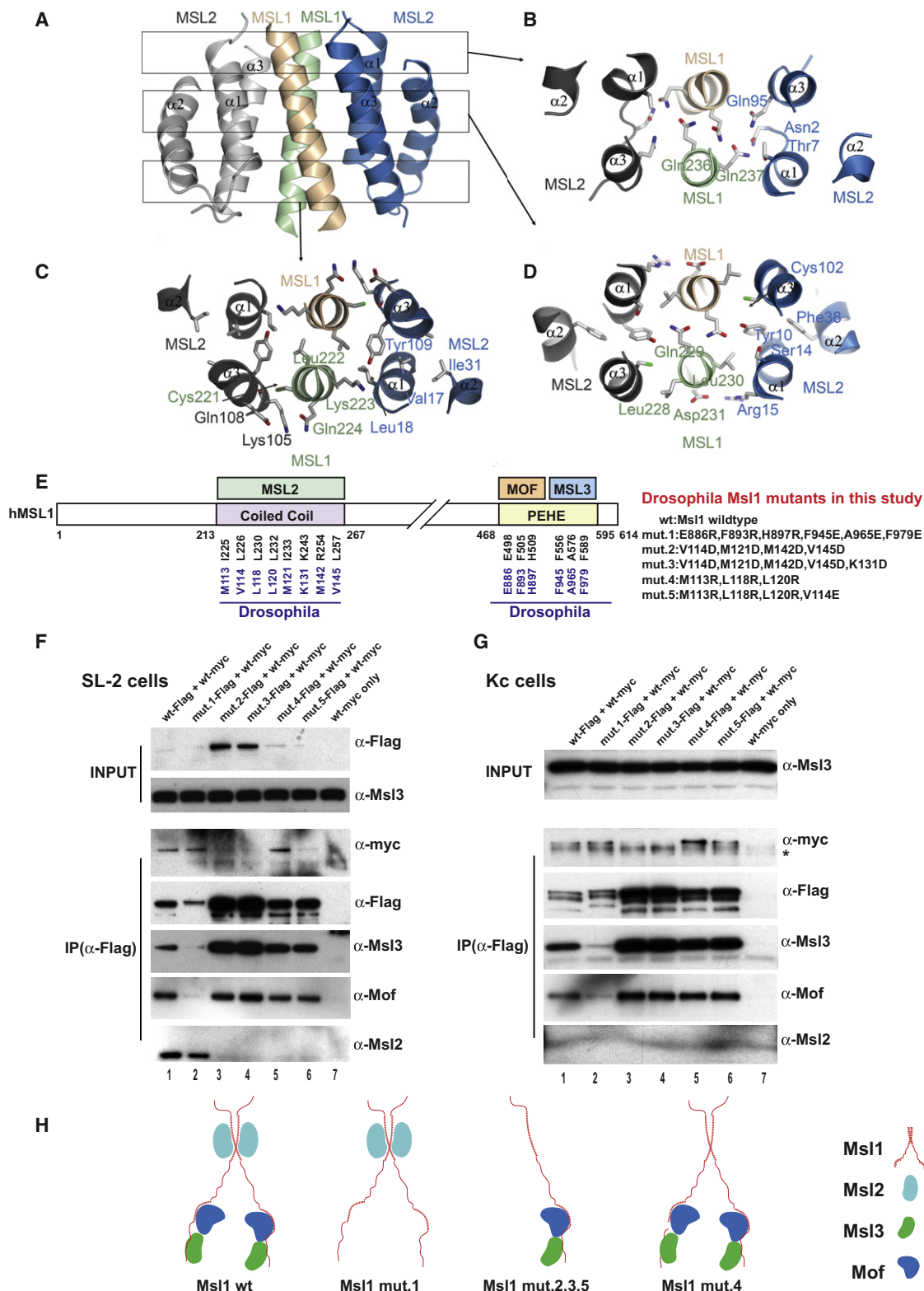
Figure 3. Details of the MSL1/MSL2 Interface and Analysis of Msl1 Derivatives in Cell Lines

(A) The helices of MSL1 and MSL2 form an antiparallel eight-helical bundle with many hydrophobic and polar interactions between the four molecules. The three details of the interface shown in (B)–(D) are localized on the structure by the black boxes.

(B) Highly conserved glutamine residues of the third heptad repeat of MSL1 (Gln236, Gln237) form several hydrogen bonds with Asn2, Thr7, and Gln95 of MSL2.

Next we designed a mutant that would not interact with Msl2 but would preserve the integrity of the Msl1 dimer. Thus, we mutated three residues in the Msl1/Msl2 interface that do not lie at *a* or *d* heptad positions to arginines (M113R, L118R, L120R: Msl1 mut.4; Figures 1F and 3E). The Msl1 mut.4 was still able to dimerize with Msl1-myc and bind Msl3 and Mof, while the interaction with Msl2 was lost (Figure 3F, lane 5), indicating that the presence of Msl2 is not required for the Msl1 dimerization. Finally, we showed that a single additional mutation in *a* heptad position (V114E) was sufficient to disrupt directly both Msl1 dimerization and Msl2 binding (Figure 3F, lane 6). Similar results were obtained when we repeated the coIP experiments with an HA-tagged WT Msl1 (Figure S3B). The hypothesis that Msl1 dimer can exist without Msl2 was further supported by coIP experiments in Kc cells, a cell culture model for *Drosophila* female cells, where Msl2 translation is inhibited (Figure 3G). The WT Msl1 dimerizes also in these cells (Figure 3G, lane 1), and similar effects as in SL-2 cells were also observed with mutants expressed in Kc cells. Interestingly, Msl1 mutants that lose the Msl2 interaction were consistently observed to be more abundant than the WT and mut.1, indicating a possible effect of Msl2 on Msl1 turnover, consistent with the in vitro ubiquitination experiment (Figures 2I and 2J). The schematic summary of the mutant Msl1-containing complexes is represented in Figure 3H. Taken together, these results conclusively show that Msl1 dimeric coiled coil is a platform for Msl2 interaction in vivo.

Msl1 Dimer Platform and Its Association with Msl2 Is Required for X Chromosome Recognition

In order to understand the importance of the Msl1 dimerization in X chromosome targeting, we tested our mutants for their interactions with chromatin by ChIP analysis in stable SL-2 cell lines. Similar expression level for each mutant was ensured by an inducible promoter (Figure S4). We used the Flag epitope for IP to selectively pull down mutant derivatives, avoiding endogenous Msl1. First we analyzed Msl1 binding to two HAS targets (roX2 and su(wa)) and several low-affinity sites within four X-linked genes (Figure 4A). Msl1 mut.1 ChIP shows that roX2 HAS binding is independent of both Msl3 and Mof, and su(wa) showed a reduced binding of the partial complex, whereas spreading across the body of the X-linked genes was completely lost. This result further supports our previous hypothesis that not all HAS are identical and show differential affinities toward various surfaces of the MSL complex (Kadlec et al., 2011). Strikingly, all the other mutants (Msl1 mut.3, mut.4, and mut.5) did not bind either to HAS or low-affinity site gene bodies. Exceptions

were observed for the promoter regions of the same genes where binding remains unaffected (see below). In order to ensure that X chromosome recognition is lost starting from the HAS, we tested 12 more HAS targets determined by Kuroda and colleagues (Alekseyenko et al., 2008) (Figure 4B). Remarkably, all the tested targets show reduced binding of Msl1 mut.1 and completely abolished binding of the Msl1 mut.3 and mut.5. The loss of binding of Msl1 mut.4 importantly shows that Msl1 dimer per se cannot target the X chromosome, but requires the composite action with Msl2. Taken together, these results clearly indicate that Msl1 dimerization-mediated Msl2 binding is necessary for the recognition of X chromosomal genes.

roX2 RNA Integration Requires the Full Complex

The MSL complex contains two functionally redundant long non-coding RNAs, roX2 and/or roX1, implicated in spreading (Franke and Baker, 1999; Meller and Rattner, 2002). However, the actual mode by which the MSL complex binds RNA remains unknown (Lee et al., 1997; Akhtar et al., 2000; Li et al., 2005; Morales et al., 2005; Fauth et al., 2010). We used Msl1 mutants to study roX integration into the complex in vivo by RNA immunoprecipitation (RIP) method, where fixed complexes are pulled down and RNAs are quantitatively measured by quantitative PCR (Selth et al., 2009). First, we optimized the RIP protocol in SL-2 cells, where roX2 but not roX1 is expressed, using the Mle subunit as a bait protein, as its interaction with roX2 is well established (Lee et al., 1997). Mle bound roX2 in vivo, as verified by two different primer pairs and did not bind a nonspecific nuclear RNA, 7SK (Figure 4C). RIP by Flag antibody gave only background levels of signal from WT SL-2 cells (Figure 4C), ensuring the specificity of signals obtained from RIP of Msl1 mutants (Figure 4D). Rox2 binding to the exogenous WT Flag-tagged Msl1 was recapitulated from the stable cell line. While Msl1 mut.1 showed a significant reduction of RNA recovery, mut.3 and mut.4 completely lost the binding despite their equivalent expression levels (Figure S4). These results indicate that Msl1-Msl3-Mof trimeric complex (Msl1 mut.3) and hexameric complex (Msl1 mut.4) cannot bind roX2 in the absence of Msl2. The Msl3 or Mof proteins are also required for complete incorporation of the RNA, but their contribution is not detectable by this method when Msl2 is not present in the complex. Msl2 thus appears to be a key subunit for stable roX2 integration into the MSL complex.

Msl1 Binds to Promoters in Male and Female Cells

Reproducible Msl1 binding to the promoters of X-chromosomal genes and its independent nature from Msl3, Mof, Msl2, and

(C) Details of the MSL1/MSL2 interactions around MSL1 Leu222. Mostly hydrophobic layer formed by MSL1 Leu222 and Ly223 and MSL2 Val17, Leu18, Tyr109, and Ile31. This layer is part of a large hydrophobic core including also MSL1 Ile225 and Leu226 and MSL2 Leu35, Leu106, and Ile110 (not shown). MSL1 Cys221 and Gln224 form several hydrogen bonds with Lys105 and Glu108 of MSL2.
(D) Glutamines 229 forming an interhelical hydrogen bond within the MSL1 dimer also interact with Tyr10 of MSL2. Leu228 and Leu230 make hydrophobic contact with MSL2. Additionally, MSL2 Arg15 forms salt bridge interactions with Asp231 and Asp233 of MSL1.
(E) Mutated residues in *Drosophila* and their human homologs are represented on the human MSL protein scheme. *Drosophila* Msl1 mutants used in this study. All Msl1 mutants, including WT, have a C-terminal 3xFlag tag.
(F) Flag immunoprecipitation of Msl1 mutants in SL-2 cells. Msl1-Flag mutants are cotransfected with WT myc-tagged Msl1, and Flag beads were used for IP. Western blots were performed with the indicated antibodies. Flag and myc tag indicates C-terminal 3xFlag and 3xMyc tag, respectively.
(G) Same experiment in (F) performed in Kc cells. Asterisk in anti-myc blot indicates a contamination band. Msl2 absence is a marker for Kc cells.
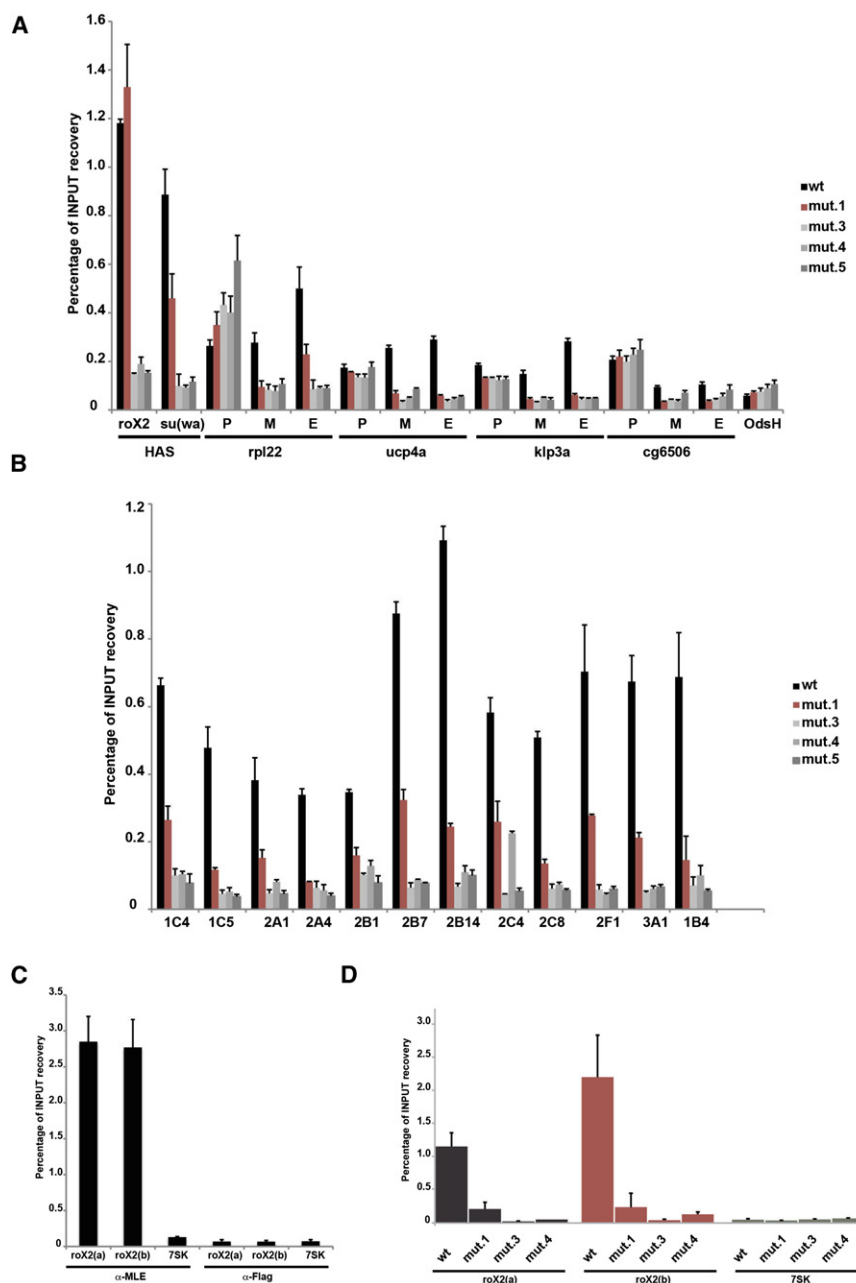(H) Schematic summary of WT or Msl1 mutants containing complexes derived from IP studies in (F) and (G).

Figure 4. Chromatin and roX2 RNA Interactions of Msl1 Mutants

(A) ChIP of Msl1 mutants with Flag antibody in SL-2 stable cell lines. Two HAS and four X-linked genes were chosen as X chromosomal targets. OdsH target is used as a negative control. P, M, and E indicate promoter, middle, and end of the genes, respectively. The error bars represent the standard deviation of three independent experiments.

(B) Same experiment as in (A) is performed on 12 selected HAS.

(C) RNA immunoprecipitation (RIP) in SL-2 cells with Mle and Flag antibody. RIP on Mle protein is used as a positive control for roX2 RNA binding. Two different roX2 sites are quantitatively amplified (roX2 a, roX2 b). 7SK is used as a nuclear RNA negative control. RIP with Flag antibody is repeated on same targets in WT SL-2 cells to show background levels of RNA recovery. The error bars represent the standard deviation of three independent experiments.

(D) Flag RIP experiment in SL-2 stable cell lines that express Msl1 mutants. Two roX2 RNA target sites and a negative control RNA target (7SK) are amplified. The error bars represent the standard deviation of three independent experiments.

males and females. Surprisingly, Msl3 was absent on autosomal promoters in male cells (Figure 5C) and on female promoters (data not shown) compared to X chromosomal targets. Msl3 occupancy at X-linked promoters was either absent or very low relative to Msl1. Taken together, these results suggest that Msl1 binding at the promoters is independent from its role in dosage compensation. The presence of Msl3 only on X chromosome ORFs provides a distinguishing feature for the X chromosomal genes versus autosomal targets with concomitant spreading of the MSL complex.

Msl1 Dimerization Is Essential for Male Viability

In order to assess the functional relevance of these *msl1* mutations in *Drosophila* in vivo, we generated transgenic flies expressing the mutant variants of *msl1* (WT Flag-tagged, mut.1, mut.3, mut.4, mut.5) in a spatiotemporally regulated manner using the UAS/Gal4 binary system. All transgenes were inserted in the same genomic location (65B2) by phiC31 integrase-mediated transformation to avoid the influence of position effects on gene expression and facilitate direct comparison upon phenotypic analysis (Groth, 2004). The fly system also enabled us to directly compare sex-specific effects of different mutations.

We first induced ectopic expression of these mutants in a WT background ubiquitously with a strong *tubulin-Gal4* driver at 25°C (Lee and Luo, 1999). Strikingly, expression of Msl1 mut.3,
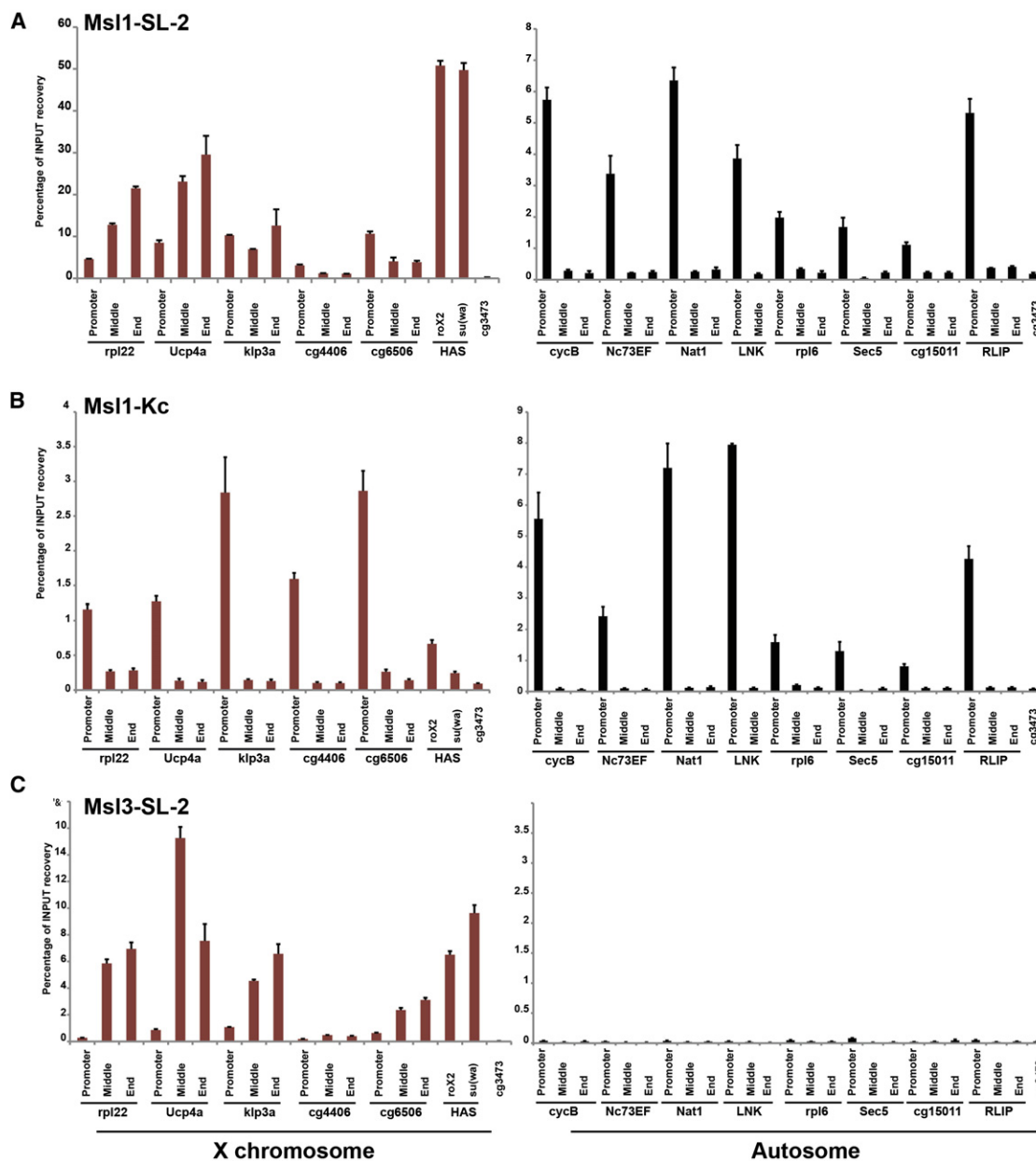
dimerization prompted us to hypothesize that this binding could be independent from its role in dosage compensation. In such a scenario, Msl1 might also be detectable at the promoters of autosomal genes, where dosage compensation does not occur. Indeed, by ChIP we detected significant enrichments at the promoters of eight random autosomal targets, while ORF binding was at the background level (Figure 5A, black bars). We also tested Msl1 chromatin interactions in female Kc cells and observed clear enrichments on the promoters of both X-linked and autosomal targets (Figure 5B). Since Mof is also present on autosomal promoters (Kind et al., 2008), we checked Msl3 systematically on the same autosomal and X-linked genes in

Figure 5. Msl1 Binds to Promoters of X and Autosomes in a Sex-Independent Manner

(A) ChIP of endogenous Msl1 in SL-2 cells. Five X-linked genes and two HAS are chosen for canonical X chromosome enrichment (red bars). Cg3473 is a negative control target site. Eight autosomal target sites are shown with black bars. The error bars represent the standard deviation of three independent experiments. Same experiment is performed for endogenous Msl1 in Kc cells (B) and endogenous Msl3 in SL-2 cells (C).

mut.4, and mut.5 caused both male and female lethality, whereas Msl1 mut.1 caused only male-specific lethality and WT Msl1 expression did not have any observable effects on viability (Figure 6A). Western blot analysis showed that Msl1 mut.3, mut.4, and mut.5, which lose Msl2 interaction, are more abundant than WT Msl1 and mut.1 (Figure 6B), as observed in our cell culture system, suggesting a possible downregulating effect of Msl2 on Msl1.

In order to ensure that lethality is not due to indirect effects of overexpression of the mutant proteins, especially for the coiled-

coil Msl1 mut.3, mut.4, and mut.5, we repeated the experiment at 18°C, where *tubulin-Gal4*-induced transgene expression can be significantly decreased relative to 25°C (Mondal et al., 2007) (Figures 6C and 6D and Figure S5). Under these conditions, we observed that female viability is restored for Msl1 mut.3 and mut.4 and partially for mut.5, whereas male-specific lethality was still observed for all mutants (except escapers for Msl1 mut.1 and mut.4). Ectopic expression of WT Msl1 in these conditions had no effects on viability. These results show that dominant-negative effects of all mutations can be observed
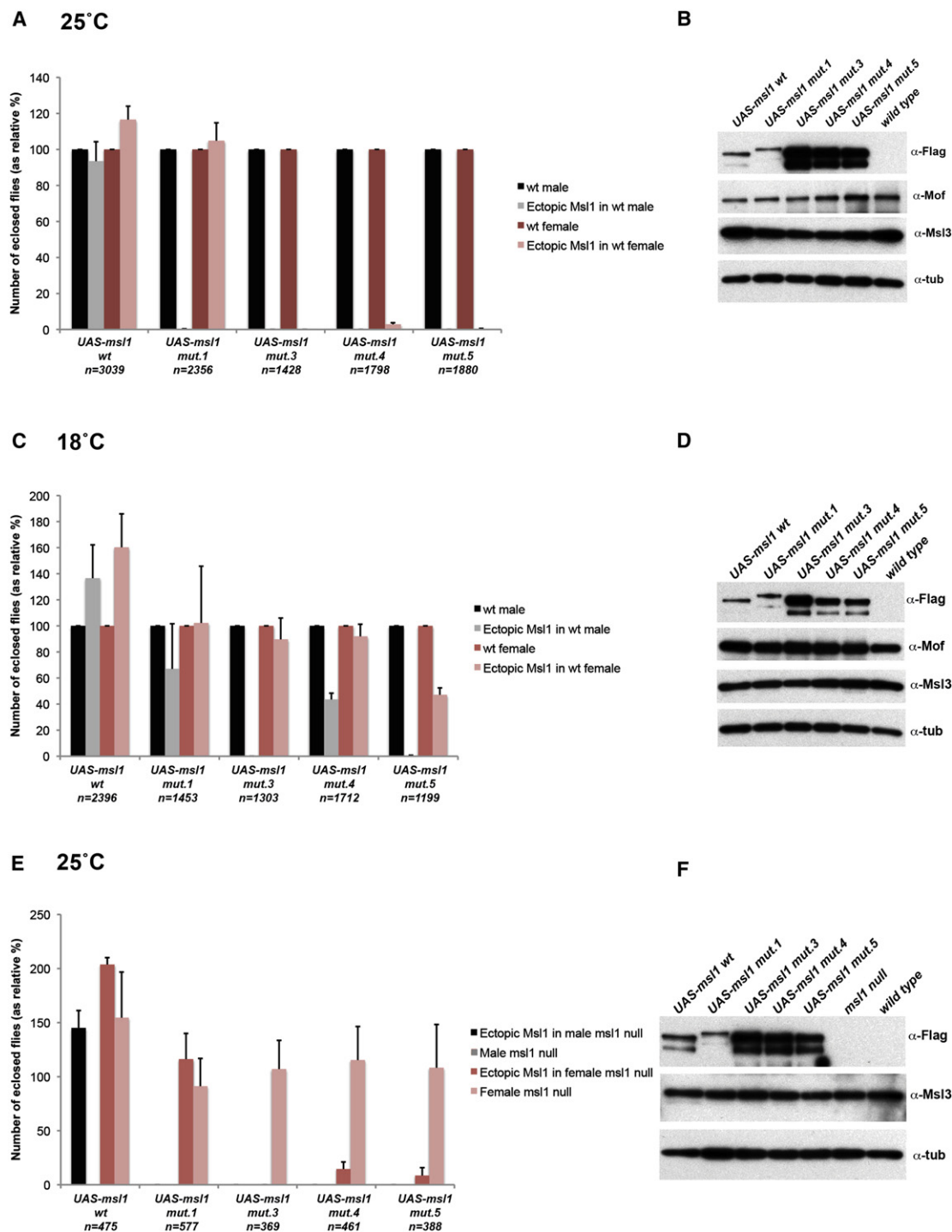
Figure 6. Viability of Adult Flies upon *tubGal4*-Induced Ectopic Expression of *UAS-msl1*

(A) Ectopic expression of WT Msl1 and Msl1 mut.1, mut.3, mut.4, and mut.5 in a WT background at 25°C. The nonexpressing *TM6Tb/UAS-msl1** (* representing Msl1 WT, mut.1, mut.3, mut.4, or mut.5) flies were used as internal controls (males, black bars; female, red bars) and scored as 100% viable. The number of eclosed *tubGal4/UAS-msl1** flies (males, gray bars; female, pink bars) expressing the *UAS-msl1** transgene are represented as relative percentages to their nonexpressing siblings. The details of the fly cross are indicated in Experimental Procedures. The total number of flies counted for each cross is indicated underneath each group. The error bars represent standard deviations of three independent crosses.

(B) Western blots from protein extracts prepared from second instar larvae carrying different *UAS-msl1** transgenes, all C-terminal 3xFlag tagged. Flag antibody was used to probe exogenous Msl1; Mof and Msl3 protein levels are shown for comparison. Tubulin levels were used as a loading control (Anti-Tubulin, DM1A, Sigma).

exclusively in males at both temperatures, whereas females become sensitive to the levels of Msl1 mut.3, mut.4, and mut.5 at 25°C.

To assess the direct effect of the mutations, we expressed the Msl1 mutant variants in *msl1*^{L60}/*msl1*^{γ269} null mutant flies to reconstitute Msl1 function. As expected, in the absence of Msl1, females are viable whereas males die as third instar larvae or at early pupal stages (Figures 6E and 6F). At 25°C, *tubulin-Gal4*-induced ectopic expression of WT Msl1 rescued completely the *msl1* loss-of-function male-specific lethality (Figure 6E). Noticeably, none of the *msl1* mutants rescued male lethality (Figure 6E). Female viability dropped significantly in Msl1 mut.3, mut.4, and mut.5, similar to the dominant effect observed upon overexpression in a WT background (Figure 6E). At 18°C, *tubulin-Gal4*-induced ectopic expression of WT Msl1 rescued the *msl1* loss-of-function male-specific lethality only partially, and other mutants failed to do so (data not shown). These results clearly show that all of the residues that are determined from the crystal structure are absolutely essential for male viability.

DISCUSSION

Msl1 and Msl2 are essential core subunits of the dosage compensation complex that contains Msl3 and Mof as well as more peripherally bound Mle. Here we report the crystal structure of the human MSL1/MSL2 subcomplex, together with a detailed biochemical and functional mutagenesis analysis in vitro and in vivo. Our study revealed several important and intriguing features of the MSL complex architecture. Contrary to the expected coiled coil-based heterodimerization with MSL2 (Li et al., 2005) we show that the MSL1 coiled-coil region mediates MSL1 homodimerization. Putative self-association of *Drosophila* Msl1 via a glycine-rich region between residues 26 and 84 was proposed by Li et al., but its oligomeric state was not further characterized (Li et al., 2005). Our data clearly show that MSL1 forms dimers, and the evolutionary nonconserved glycine-rich region is dispensable for this interaction. The MSL1 dimeric coiled coil then binds two molecules of MSL2, forming a heterotetrameric core of the MSL complex. The structural data as well as immunoprecipitation experiments demonstrate that the Msl1 dimerization is required for the interaction with Msl2, since the single Msl1 molecule contains only half of the Msl2 binding site. The fact that the Msl1 dimerization can be observed in female cells, lacking Msl2, suggests that Msl2 is not required for the Msl1 dimer formation. This was additionally confirmed by mutagenesis of the Msl2 binding surface on Msl1.

Finally, we show that both Msl1 dimerization and Msl2 binding are independent of the presence of Msl3 or Mof. Importantly, since all our structure-based Msl1 mutations specifically affect only the targeted interfaces, without influencing interaction with other MSL proteins and gene promoters, we believe that they do not significantly perturb the overall structure of Msl1 that is anyhow predicted to be mostly intrinsically disordered. We had reported earlier that MSL1 interacts with MSL3 and MOF with relatively short segments (20 and 40 residues, respectively), while the surrounding regions are poorly conserved and predicted to be unstructured (Kadlec et al., 2011). Consistent with this, the MSL1/MSL2 structure reveals yet another short, highly conserved region that is used both for MSL1 dimerization and the MSL2 binding, further reinforcing the scaffolding role of MSL1.

Msl1 and X Chromosome Recognition

Using our Msl1 mutants, we are able to create partial complexes and assess specifically the role of individual MSL subunits. We found that Msl1 per se cannot recognize X chromosomal features other than promoters (Figure S6). However, binding of Msl2 to the Msl1 dimer has two important consequences: rudimentary recognition of X chromosome and roX2 RNA integration into the complex. It is clear that HAS are not identical in terms of their affinity to the complex. Msl1 mut.1 ChIP experiment shows that roX2 HAS only requires Msl1/Msl2 while all other tested HAS show reduced level of the complex. We propose that chromatin regions like roX2 HAS are the "elementary high-affinity sites" where initial enrichment of Msl1 on X chromosome is mediated by a common action of Msl1/Msl2.

Our RIP results show that Msl1-Mof-Msl3 trimer or hexamer (corresponding to Msl1 mut.3 and mut.4) cannot bind roX RNA, indicating an active role of Msl2 in the binding. Loss of RNA signal in RIP experiments cannot be due to a loss of interaction with Mle, as Mle association with the complex is bridged by RNA (Richter et al., 1996; Copps et al., 1998; Smith et al., 2000). Interestingly, Msl1 mut.1 also shows significant loss of roX RNA interaction, implying that full integration happens only in the context of the whole complex. It is tempting to speculate that roX2 RNA interaction may enable crosstalk between the two distant N-terminal Msl1/Msl2 and C-terminal Msl1-Msl3-Mof catalytic centers of the MSL complex.

Dimerization of Msl1 Enables Spreading of the Complex along Gene Bodies

The fact that MSL1 dimerizes through such an extended interface (buried surface of 1340 Å²) and the dimer formation is

---

(C) Recovery of female but not male viability upon weaker/lower ectopic expression of Msl1 mut.3, mut.4, and mut.5 in a WT background at 18°C. Crosses were performed as in (A), but the flies had been kept at 18°C.

(D) Western blots were done as in (B).

(E) Male lethality rescue assay by ectopic expression of WT Msl1 and Msl1 mut.1, mut.3, mut.4, and mut.5 in *msl1* null (*msl1*^{L60}/*msl1*^{γ269}) background at 25°C. The number of eclosed *msl1*^{L60}/*msl1*^{γ269}; *tubGal4/UAS-msl1** flies (males, black bars; females, red bars) expressing the *UAS-msl1** transgene in *msl1* null mutant background are represented as relative percentages to their nonexpressing heterozygous siblings (*msl1*^{L60 or γ269} /CyO, GFP; UAS-msl1*/TM6Tb). The non-expressing *msl1* null siblings (*msl1*^{L60}/*msl1*^{γ269}; UAS-msl1*/TM6Tb) (males, gray bars; females, pink bars) are shown as internal controls for the male-specific lethality of *msl1* loss of function. The cross is indicated in Experimental Procedures. The error bars represent standard deviations of three independent crosses.

(F) Tubulin antibody was used for loading control and Msl3 and Flag antibodies were probed to show the levels of expression of transgenic Msl1 and endogenous Msl3.

required for MSL2 binding dramatically changes our view on the dosage compensation complex structure and assembly. As it is possible to copurify the recombinant human MSL1/MSL2/MSL3/MOF complex from insect cells using Flag-tagged MSL2 (Wu et al., 2011) that can presumably only bind dimeric MSL1, it is very likely that the MSL complex contains all the subunits in pairs, including also MSL3 and MOF. We therefore propose that MSL complex binding to the open reading frames of the X-linked genes in *Drosophila* could happen through a dimer-dependent nucleosome engagement rather than via Msl1-mediated oligomerization of MSL complexes on chromatin (Li et al., 2005) (Figure S6). The presence of two copies of each of the chromatin-modifying or modification-binding domains of the complex would increase the number of possible, probably transient contacts with nucleosome(s), containing histones also in pairs. The *Drosophila* Msl1 scaffold is a large, mostly disordered protein (1039 residues) that provides the MSL complex with a high degree of flexibility. The Msl2 and Mof/Msl3 binding regions of Msl1 are separated by 720 poorly conserved, probably unstructured residues. It is thus possible that while some subunits are attached to chromatin, others, connected by the flexible Msl1 linker, can browse the surrounding nucleosomes for new attracting histone marks. The dimer-dependent spreading can also be deduced from the ChIP analysis of Msl3/Mof-deficient Msl1 mutant in the endogenous Msl1 background (Figure 4A). This mutant can still dimerize with the endogenous intact Msl1, albeit at low levels observed from our IP analysis (Figure 3F); however, it cannot spread to the open reading frames, which indicates that both copies of Msl3 and Mof are required for spreading.

Sex-Independent Binding of Msl1 at Promoters

The occurrence of Msl1 at the promoters in both sexes and its independence from other members of the complex for this binding suggests the possibility of an evolutionarily conserved function in higher eukaryotes. All complex members, except for Msl2 and Msl1, have origins traceable to yeast (Marín, 2003). The emergence of "Msl1-like genes," namely Msl1 and Nsl1 in *Drosophila*, both having a PEHE region to bind Mof through the same surface (Kadlec et al., 2011), seems to focus this ubiquitous acetyltransferase to promoter regions of a large portion of the *Drosophila* genome. Indeed, Mof binds to promoters in both sexes and is responsible for the promoter chromatin H4K16 acetylation (Kind et al., 2008). It was also observed that RNAi of Nsl1 or Msl1 does not completely diminish Mof occupancy at the promoter, probably because both proteins have complementary roles (Raja et al., 2010). It will be interesting to delineate possible functional interplay of Msl1 and Nsl1 at promoters as well as the distribution of Mof between these two proteins. It is important to note that Msl1 is not essential for female viability, possibly due to this redundancy between Msl1 and Nsl1 in terms of Mof recruitment to the promoters. Female viability decreases only when Msl1 mutants that have an intact PEHE region are expressed, probably causing mistargeting of Mof. In addition, no effect is observed upon expression of WT Msl1 or mut.1, strengthening the hypothesis that the observed female phenotypes are due to Mof rather than Msl1. One distinguishing

factor between the promoter complex and the dosage compensation complex is Msl3, whose binding on the autosomal promoters was undetectable and on X-linked promoters was also very low.

In summary, our study enhances our perspective on the architecture of MSL complex and how this configuration could help spreading of MSL complex on the X chromosome. Future structural work incorporating the remaining MSL complex subunits, including RNA, is likely to reveal novel insights into the molecular mechanisms underlying this chromatin-binding complex.

EXPERIMENTAL PROCEDURES

Expression, Purification, and Crystallization

A His-tag fusion of a proteolytically stable fragment of the human MSL1 coiled-coli region (residues 213–267) and untagged N-terminal domain of MSL2$_{1-116}$ was coexpressed in bacteria. The purified complex crystallized in a solution containing 0.1 M HEPES (pH 7.0), 1.1 M sodium malonate (pH 6.5), and 0.8% Jeffamine ED 2001. The complex of MSL1$_{213-252}$ and MSL2$_{1-116}$ was produced in the same way, and crystals were obtained in 0.1 M MES (pH 6.0) and 1.6 M ammonium sulfate.

Data Collection and Structure Determination

The structure of the MSL1$_{213-267}$/MSL2$_{1-116}$ was solved by a zinc multiple anomalous dispersion (MAD) experiment and was refined to R factor of 25.6% and R$_{free}$ of 29.6% (Table 1) with all residues in allowed (96.5% in favored) regions of the Ramachandran plot, as analyzed by MOLPROBITY (Davis et al., 2004). The structure of the MSL1$_{213-254}$/MSL2$_{1-116}$ was solved by molecular replacement using PHASER (McCoy et al., 2005) and the MSL1/MSL2 model obtained above as a search model. The structure was refined using Refmac5 (with TLS refinement) to R factor of 24.4% and R$_{free}$ of 26%. All the residues are in allowed (96% in favored) regions of the Ramachandran plot. A representative part of the 2F$_o$ − F$_c$ electron density map calculated using the refined model is shown in Figure S7. Details of the crystallography procedures are available in Supplemental Experimental Procedures.

Flag Immunoprecipitations

Harvested cells were washed with cold PBS two times and resuspended in 1 ml HEMGT 150 (25 mM HEPES/NaOH 7.6, 0.1 mM EDTA, 12.5 mM MgCl$_2$, 10% glycerol, 0.2% Tween-20, 150 mM NaCl, supplemented with protease inhibitor cocktail from Roche) buffer. After three freeze/thaw cycles in liquid N$_2$ and 37°C water bath, the extract was centrifuged for 30 min at 20,000× g. A bed volume of 30 μl M2-Flag agarose beads (Sigma) was incubated for 3 hr at 4°C. The beads were washed five times in HEMGT 250 and boiled with 40 μl 4X Laemmli Buffer.

Chromatin Immunoprecipitation in SL-2 Cells

ChIP was carried out as described in Kadlec et al., 2011 with a few modifications based on Chelex protocol adapted from Nelson et al., 2009. Details are available in Supplemental Experimental Procedures.

RNA Immunoprecipitation

RIP was carried out as described in Selth et al., 2009 with 25 million SL-2 stable lines that had been induced with CuSO$_4$ for 12 hr with indicated amounts in Figure S4.

Drosophila Crosses

In order to obtain flies ectopically expressing mutant *msl1* in a WT background, *y¹ w*; P{tubP-GAL4}LL7/ TM6B, P{Ubi-GFP.S65T}PAD2, Tb¹* virgin females were crossed with males homozygous for the appropriate *UAS-msl1** transgenic insertion. For analysis in *msl1* null mutant background, *y¹ w*; msl1^L60^/ CyO, P{ActGFP}JMR1; P{tubP-GAL4}LL7/ TM6B, Tb¹* virgin females were

Table 1. Data Collection and Refinement Statistics

	MSL1$_{213-252}$ MSL2$_{1-116}$	MSL1$_{213-267}$ MSL2$_{1-116}$	Peak	Inflection point	Remote
Data collection					
Space group	$P3_221$	$P2_12_12$	$P2_12_12$	$P2_12_12$	$P2_12_12$
Cell dimensions					
a, b, c (Å)	101, 101, 88.6	104.6, 182.2, 89.5	104.1, 180.60, 89.4	104.3, 180.8, 89.7	104.8, 181.7, 90.3
α, β, γ (°)	90, 90, 120	90, 90, 90	90, 90, 90	90, 90, 90	90, 90, 90
Resolution (Å)	31–3.25 (3.37–3.25)[a]	50–3.5 (3.65–3.5)	50–3.6 (3.73–3.6)	50–3.65 (3.75–3.65)	50–3.7 (3.83–3.7)
R$_{merge}$	6.6 (68)	7.3 (72)	6.8 (77)	6.6 (77)	6.8 (78)
I/σI	11.6 (1.9)	11 (1.8)	14.5 (1.9)	14.8 (1.9)	14.4 (1.9)
Completeness (%)	98.7 (99.9)	97.2 (98.2)	99.8 (99)	99.9 (99.9)	99.6 (96.4)
Redundancy	3.6 (3.8)	3.7 (3.7)	3.9 (3.9)	3.9 (3.9)	3.9 (3.7)
Refinement					
Resolution (Å)	31–3.25	45–3.5	–	–	–
No. reflections	8,005	20,450	–	–	–
R$_{work}$/R$_{free}$	24.4/26	25.6/29.6	–	–	–
No. atoms					
Protein	2,260	7,030	–	–	–
Zn ion	4	12	–	–	–
B factors					
Protein	57	79	–	–	–
Zn ion	72	84	–	–	–
Rmsds					
Bond lengths (Å)	0.009	0.007	–	–	–
Bond angles (°)	1.042	0.956	–	–	–

[a]Values in parentheses are for highest-resolution shell.

crossed with y^1 w^*; msl1$^{\gamma 269}$ cn^1 bw^1/CyO, P{ActGFP}JMR1; P{UAS-msl1*} 65B2 males.

ACCESSION NUMBERS

Coordinates of MSL1$_{213-267}$/MSL2$_{1-116}$ and MSL1$_{213-254}$/MSL2$_{1-116}$ have been deposited to the Protein Data Bank with accession codes 4B86 and 4B7Y, respectively.

SUPPLEMENTAL INFORMATION

Supplemental Information includes seven figures, one table, and Supplemental Experimental Procedures and can be found with this article online at http://dx.doi.org/10.1016/j.molcel.2012.09.014.

ACKNOWLEDGMENTS

REFERENCES

Akhtar, A., and Becker, P.B. (2000). Activation of transcription through histone H4 acetylation by MOF, an acetyltransferase essential for dosage compensation in Drosophila. Mol. Cell 5, 367–375.

Akhtar, A., Zink, D., and Becker, P.B. (2000). Chromodomains are protein-RNA interaction modules. Nature 407, 405–409.

Alekseyenko, A.A., Peng, S., Larschan, E., Gorchakov, A.A., Lee, O.-K., Kharchenko, P., McGrath, S.D., Wang, C.I., Mardis, E.R., Park, P.J., and Kuroda, M.I. (2008). A sequence motif within chromatin entry sites directs MSL establishment on the Drosophila X chromosome. Cell 134, 599–609.

Alvarez, S.E., Harikumar, K.B., Hait, N.C., Allegood, J., Strub, G.M., Kim, E.Y., Maceyka, M., Jiang, H., Luo, C., Kordula, T., et al. (2010). Sphingosine-1-phosphate is a missing cofactor for the E3 ubiquitin ligase TRAF2. Nature 465, 1084–1088.

Augui, S., Nora, E.P., and Heard, E. (2011). Regulation of X-chromosome inactivation by the X-inactivation centre. Nat. Rev. Genet. 12, 429–442.

Borden, K.L., Boddy, M.N., Lally, J., O'Reilly, N.J., Martin, S., Howe, K., Solomon, E., and Freemont, P.S. (1995). The solution structure of the RING finger domain from the acute promyelocytic leukaemia proto-oncoprotein PML. EMBO J. 14, 1532–1541.

Brzovic, P.S., Rajagopal, P., Hoyt, D.W., King, M.C., and Klevit, R.E. (2001). Structure of a BRCA1-BARD1 heterodimeric RING-RING complex. Nat. Struct. Biol. 8, 833–837.

Budhidarmo, R., Nakatani, Y., and Day, C.L. (2012). RINGs hold the key to ubiquitin transfer. Trends Biochem. Sci. 37, 58–65.

Conrad, T., and Akhtar, A. (2011). Dosage compensation in Drosophila melanogaster: epigenetic fine-tuning of chromosome-wide transcription. Nat. Rev. Genet. 13, 123–134.

Conrad, T., Cavalli, F.M.G., Holz, H., Hallacli, E., Kind, J., Ilik, I., Vaquerizas, J.M., Luscombe, N.M., and Akhtar, A. (2012a). The MOF chromobarrel domain controls genome-wide H4K16 acetylation and spreading of the MSL complex. Dev. Cell 22, 610–624.

Conrad, T., Cavalli, F.M.G., Vaquerizas, J.M., Luscombe, N.M., and Akhtar, A. (2012b). Drosophila dosage compensation involves enhanced Pol II recruitment to male X-linked promoters. Science 337, 742–746.

Copps, K., Richman, R., Lyman, L.M., Chang, K.A., Rampersad-Ammons, J., and Kuroda, M.I. (1998). Complex formation by the Drosophila MSL proteins: role of the MSL2 RING finger in protein complex assembly. EMBO J. 17, 5409–5417.

Davis, I.W., Murray, L.W., Richardson, J.S., and Richardson, D.C. (2004). MOLPROBITY: structure validation and all-atom contact analysis for nucleic acids and their complexes. Nucleic Acids Res. 32(Web Server issue), W615–W619.

Deng, X., Hiatt, J.B., Nguyen, D.K., Ercan, S., Sturgill, D., Hillier, L.W., Schlesinger, F., Davis, C.A., Reinke, V.J., Gingeras, T.R., et al. (2011). Evidence for compensatory upregulation of expressed X-linked genes in mammals, Caenorhabditis elegans and Drosophila melanogaster. Nat. Genet. 43, 1179–1185.

Fauth, T., Müller-Planitz, F., König, C., Straub, T., and Becker, P.B. (2010). The DNA binding CXC domain of MSL2 is required for faithful targeting the Dosage Compensation Complex to the X chromosome. Nucleic Acids Res. 38, 3209–3221.

Franke, A., and Baker, B.S. (1999). The rox1 and rox2 RNAs are essential components of the compensasome, which mediates dosage compensation in Drosophila. Mol. Cell 4, 117–122.

Gelbart, M.E., and Kuroda, M.I. (2009). Drosophila dosage compensation: a complex voyage to the X chromosome. Development 136, 1399–1410.

Groth, A.C. (2004). Construction of Transgenic Drosophila by Using the Site-Specific Integrase From Phage C31. Genetics 166, 1775–1782.

Hallacli, E., and Akhtar, A. (2009). X chromosomal regulation in flies: when less is more. Chromosome Res. 17, 603–619.

Hilfiker, A., Hilfiker-Kleiner, D., Pannuti, A., and Lucchesi, J.C. (1997). mof, a putative acetyl transferase gene related to the Tip60 and MOZ human genes and to the SAS genes of yeast, is required for dosage compensation in Drosophila. EMBO J. 16, 2054–2060.

Ilik, I., and Akhtar, A. (2009). roX RNAs: non-coding regulators of the male X chromosome in flies. RNA Biol. 6, 113–121.

Kadlec, J., Hallacli, E., Lipp, M., Holz, H., Sanchez-Weatherby, J., Cusack, S., and Akhtar, A. (2011). Structural basis for MOF and MSL3 recruitment into the dosage compensation complex by MSL1. Nat. Struct. Mol. Biol. 18, 142–149.

Kharchenko, P.V., Xi, R., and Park, P.J. (2011). Evidence for dosage compensation between the X chromosome and autosomes in mammals. Nat. Genet. 43, 1167–1169, author reply 1171–1172.

Kind, J., Vaquerizas, J.M., Gebhardt, P., Gentzel, M., Luscombe, N.M., Bertone, P., and Akhtar, A. (2008). Genome-wide analysis reveals MOF as a key regulator of dosage compensation and gene expression in Drosophila. Cell 133, 813–828.

Kruse, J.-P., and Gu, W. (2009). MSL2 promotes Mdm2-independent cytoplasmic localization of p53. J. Biol. Chem. 284, 3250–3263.

Lee, T., and Luo, L. (1999). Mosaic analysis with a repressible cell marker for studies of gene function in neuronal morphogenesis. Neuron 22, 451–461.

Lee, C.G., Chang, K.A., Kuroda, M.I., and Hurwitz, J. (1997). The NTPase/helicase activities of Drosophila maleless, an essential factor in dosage compensation. EMBO J. 16, 2671–2681.

Li, F., Parry, D.A.D., and Scott, M.J. (2005). The amino-terminal region of Drosophila MSL1 contains basic, glycine-rich, and leucine zipper-like motifs that promote X chromosome binding, self-association, and MSL2 binding, respectively. Mol. Cell. Biol. 25, 8913–8924.

Marín, I. (2003). Evolution of chromatin-remodeling complexes: comparative genomics reveals the ancient origin of "novel" compensasome genes. J. Mol. Evol. 56, 527–539.

McCoy, A.J., Grosse-Kunstleve, R.W., Storoni, L.C., and Read, R.J. (2005). Likelihood-enhanced fast translation functions. Acta Crystallogr. D Biol. Crystallogr. 61, 458–464.

Meller, V.H., and Rattner, B.P. (2002). The roX genes encode redundant male-specific lethal transcripts required for targeting of the MSL complex. EMBO J. 21, 1084–1091.

Mondal, K., Dastidar, A.G., Singh, G., Madhusudhanan, S., Gande, S.L., VijayRaghavan, K., and Varadarajan, R. (2007). Design and isolation of temperature-sensitive mutants of Gal4 in yeast and Drosophila. J. Mol. Biol. 370, 939–950.

Morales, V., Regnard, C., Izzo, A., Vetter, I., and Becker, P.B. (2005). The MRG domain mediates the functional integration of MSL3 into the dosage compensation complex. Mol. Cell. Biol. 25, 5947–5954.

Nelson, J., Denisenko, O., and Bomsztyk, K. (2009). The fast chromatin immunoprecipitation method. Methods Mol. Biol. 567, 45–57.

Raja, S.J., Charapitsa, I., Conrad, T., Vaquerizas, J.M., Gebhardt, P., Holz, H., Kadlec, J., Fraterman, S., Luscombe, N.M., and Akhtar, A. (2010). The nonspecific lethal complex is a transcriptional regulator in Drosophila. Mol. Cell 38, 827–841.

Richter, L., Bone, J.R., and Kuroda, M.I. (1996). RNA-dependent association of the Drosophila maleless protein with the male X chromosome. Genes Cells 1, 325–336.

Scott, M.J., Pan, L.L., Cleland, S.B., Knox, A.L., and Heinrich, J. (2000). MSL1 plays a central role in assembly of the MSL complex, essential for dosage compensation in Drosophila. EMBO J. 19, 144–155.

Selth, L.A., Gilbert, C., and Svejstrup, J.Q. (2009). RNA immunoprecipitation to determine RNA-protein associations in vivo. Cold Spring Harb. Protoc. 2009, t5234.

Smith, E.R., Pannuti, A., Gu, W., Steurnagel, A., Cook, R.G., Allis, C.D., and Lucchesi, J.C. (2000). The drosophila MSL complex acetylates histone H4 at lysine 16, a chromatin modification linked to dosage compensation. Mol. Cell. Biol. 20, 312–318.

Smith, E.R., Cayrou, C., Huang, R., Lane, W.S., Côté, J., and Lucchesi, J.C. (2005). A human protein complex homologous to the Drosophila MSL complex is responsible for the majority of histone H4 acetylation at lysine 16. Mol. Cell. Biol. 25, 9175–9188.

Uchiki, T., Kim, H.T., Zhai, B., Gygi, S.P., Johnston, J.A., O'Bryan, J.P., and Goldberg, A.L. (2009). The ubiquitin-interacting motif protein, S5a, is ubiquitinated by all types of ubiquitin ligases by a mechanism different from typical substrate recognition. J. Biol. Chem. 284, 12622–12632.

Wu, L., Zee, B.M., Wang, Y., Garcia, B.A., and Dou, Y. (2011). The RING finger protein MSL2 in the MOF complex is an E3 ubiquitin ligase for H2B K34 and is involved in crosstalk with H3 K4 and K79 methylation. Mol. Cell 43, 132–144.

Zheng, N., Wang, P., Jeffrey, P.D., and Pavletich, N.P. (2000). Structure of a c-Cbl-UbcH7 complex: RING domain function in ubiquitin-protein ligases. Cell 102, 533–539.